# Remote Comparison of Two Sr Optical Lattice Clocks through a 58 km Fiber Link

Tang-Yin Liao(廖堂银)[1,2,3], Hao Liu(刘豪)[1,3,4], Fei Meng(孟飞)[1,3], Qiang Wang(王强)[1,3,5], Tao Yang(杨涛)[1,3], Hao-Chen Tian(田昊晨)[1,3], Bing-Kun Lu(卢炳坤)[1,3], Lin Zhu(朱琳)[1,2,3], Ye Li(李烨)[1,3], Bai-Ke Lin(林百科)[1,3], Zhan-Jun Fang(方占军)[1,3,5], and Yi-Ge Lin(林弋戈)[1,3,5*]

[1]*Division of Time and Frequency Metrology, National Institute of Metrology, Beijing 100029, China*
[2]*Department of Precision Instrument, Tsinghua University, Beijing 100084, China*
[3]*Key Laboratory of Time Frequency and Gravity Primary Standard, State Administration for Market Regulation, Beijing 100029, China*
[4]*Institute of Precision Optical Engineering, School of Physics Science and Engineering, Tongji University, Shanghai 200092, China*
[5]*Hefei National Laboratory, Hefei 230088, China*

(Received 16 January 2025; accepted manuscript online 17 February 2025)

Two $^{87}$Sr optical lattice clocks (OLCs) are being developed and operated at the National Institute of Metrology (NIM), located on different campuses that are 40 km apart. In order to compare the optical frequencies of these two Sr OLCs, a 58-km noise canceled fiber link is built to transfer both a 1542-nm transfer laser and a microwave reference from Changping campus to Hepingli campus. Two commercial optical frequency combs (OFCs) with adapted single-branch 698/1542 nm outputs coherently unite the two 698-nm clock lasers and the 1542-nm transfer laser. The fractional instability of the comparison yields $3.1\times10^{-17}$ at 10000 s averaging time. The measured fractional frequency difference between these two Sr OLCs was evaluated to be $1.9(3.2)\times10^{-17}$, which is within their claimed uncertainties. This result demonstrates the consistency of their frequencies when they serve as optical frequency standards. Our remote comparison demonstrates the feasibility of optical clock comparison through a long-distance fiber link and contributes to the progress of redefinition of the SI second.

DOI: 10.1088/0256-307X/42/3/034201 CSTR: 32039.14.0256-307X.42.3.034201

*1. Introduction.* Optical frequency standards (OFSs) achieved unprecedented high accuracy in the last 10 years.[1–6] The systematic frequency shift uncertainties of these best OFSs have entered $10^{-19}$ level,[7–9] and significantly surpassed those of the best cesium primary frequency standards which reproduced the time unit of the International system of units (SI), the second. The Consultative Committee for Time and Frequency (CCTF) of the International Committee for Weights and Measures (CIPM) has been considering to redefine the SI second based on OFSs for a long time, and released the roadmap towards the redefinition of the second in 2024.[10] In this roadmap, mandatory criteria that must be fulfilled before the redefinition of the second have been defined. The first and most important criterion is to verify the accuracy budgets of the OFSs. For most accurate OFSs, it is not possible to find a better frequency standard to measure their performance. Comparisons between these OFSs are the most effective method to verify their accuracy budgets.[1,5,11–20]

It is straightforward to make a comparison between OFSs of the same type, like two Sr optical lattice clocks (OLCs), in the same laboratory. In this case, the frequency differences can be directly calculated or measured from the acoustic-optic modulators (AOMs) frequencies that adopted to lock the clock transitions, without the necessity of introducing optical frequency combs. But for a remote comparison of OFSs, tightly phase-locked OFCs and long-distance optical frequency transfer link are required.[16]

Fiber links have been applied to transfer optical frequencies to remote sites without degrading the accuracy of the OFSs.[21–25] In order to take advantage of the commercial communication optical fiber networks, a transfer laser at the communication band inherits the frequency accuracy of the OFSs assisted by broadband OFCs serving as a precise optical clockwork. After being transferred to the remote sites through the long noise-cancelled fiber link, the frequency difference between the two OFSs can be accessed with the help of the second OFC at the remote site.[12] Based on this scheme, in this work, we experimentally demonstrate a remote comparison of two Sr OLCs through a 58-km communication optical fiber link and two OFCs yielding a measured fractional frequency difference of $1.9(3.2)\times10^{-17}$.

The general schematic experimental setup of the whole comparison system is shown in Fig. 1. Two $^{87}$Sr OLCs are being developed at NIM. NIM-Sr1 is the first Sr OLC developed on NIM Hepingli campus.[26] NIM-Sr2 is the

*Corresponding author. Email: linyige@nim.ac.cn
© 2025 Chinese Physical Society and IOP Publishing Ltd. All rights, including for text and data mining, AI training, and similar technologies, are reserved.

other Sr OLC developed on NIM Changping campus.[27] Two OFCs located on the two campus, $\mathrm{OFC_{hpl}}$, and $\mathrm{OFC_{chp}}$, work as two optical clockworks that transfer the accuracy of Sr OLCs to 1542-nm region. A transfer laser at 1542 nm connects the two OFCs through a 58 km fiber link with active fiber noise cancellation (FNC). The 10 MHz microwave frequency reference $f_{\mathrm{ref.chp}}$ is from a H-maser (VCH-1003M, No. 4857, VREMYA-CH) located on Changping campus. The microwave reference $f_{\mathrm{ref,\,hpl}}$ is delivered to Hepingli campus by another FNC unit (transmitter FNC1T and receiver FNC1R, homemade).[28] This exploits state-of-the-art microwave frequency transfer over fiber technique utilizing 1555-nm laser as optical carrier. Wavelength division multiplexing (WDM) devices allows the fiber link to transfer both the 1542-nm transfer laser and the 1555-nm laser through the same fiber core.

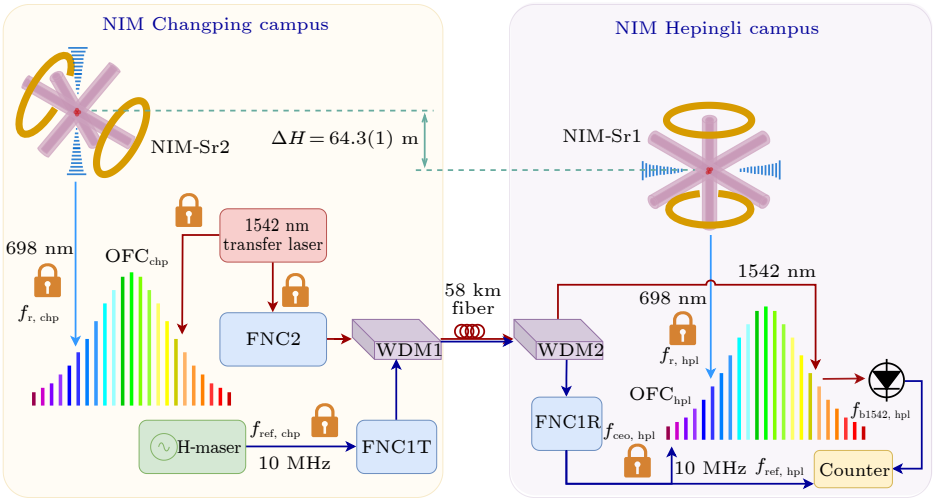


**Fig. 1.** The schematic experimental setup for the frequency comparison of two Sr optical lattice clocks. OFC: optical frequency comb, FNC: fiber noise cancellation, WDM: wavelength division multiplexing.

NIM-Sr1 is a Sr OLC with an almost horizontal one-dimensional (1D) optical lattice.[29] After its first evaluation in 2015,[26] many improvements have been implemented. A clock laser based on a 30 cm ultra-low expansion (ULE) glass reference cavity was built. Time interleaved self-comparison showed a short term instability of $3.2\times10^{-16}$.[30] The lattice laser frequency is lock to $\mathrm{OFC_{hpl}}$ to precisely meet the magic wavelength. The blackbody radiation (BBR) frequency shift is evaluated by accurately measuring the environmental temperature seen by the atoms with carefully calibrated temperature sensor arrays. In 2021, the total systematic frequency shift uncertainty of NIM-Sr1 was evaluated to be $2.9\times10^{-17}$.[31] The absolute frequency of NIM-Sr1 is measured against the ensemble of primary and secondary frequency standards published in the Circular T bulletin through a satellite link. The results indicate that the measured absolute frequency of NIM-Sr1 is consistent with the international recommendation frequency of $^{87}$Sr clock transition.

NIM-Sr2 has a nearly vertical 1D optical lattice. It has a Zeeman slower with a magnetic field that is generated by ring-shaped permanent magnets, which completely eliminates the heat generated by traditional coils.[32] Some other methods were also applied to improve the temperature homogeneity around the magneto-optical trap (MOT) area.[27] The BBR shift of NIM-Sr2 is reduced to less than $5\times10^{-18}$. The cooling lasers and lattice laser frequencies are stabilized to high finesse optical cavities. The repumping lasers are referenced to a wavemeter (WS-U, Highfinesse). These lasers are delivered to the MOT by fibers and optics installed in cage systems, which helps to improve the robustness of the laser system. The 698-nm clock laser of NIM-Sr2 is based on another 30 cm ULE reference cavity installed on Changping campus. This clock laser has a similar performance as NIM-Sr1's clock laser with an instability of $2 \sim 3 \times 10^{-16}$ at 1 s. In order to obtain sufficient laser power for atom interrogation, Sr–Sr comparison and Sr–$\mathrm{Ca^+}$ comparison, the power of the clock laser is amplified to 34 mW by injection locking of a laser diode. A Ti:sapphire comb based optical frequency divider developed by East China Normal University has been transported to our lab.[33] It compares NIM-Sr2 with a $\mathrm{Ca^+}$ OFS located in the same lab developed by the Innovation Academy for Precision Measurement Science and Technology of the Chinese Academy of Sciences.[34] This comparison helps to evaluate some of the systematic shifts of NIM-Sr2.

The commercial Er:fiber OFC (DFC, TOPTICA), $\mathrm{OFC_{chp}}$, has a single-branch type 698/1542 nm output. The repetition rate of the OFC, $f_{\mathrm{r,\,chp}}$, is $\sim 200$ MHz. Its carrier envelop offset frequency, $f_{\mathrm{ceo,\,chp}}$, is naturally cancelled through difference frequency generation leading to a zero $f_{\mathrm{ceo}}$. The previous analysis of the uncertainty of the $f_{\mathrm{ceo}}$ proves that the passive stabilized $f_{\mathrm{ceo}}$ has negligible influence on the accuracy of the frequency comparison between the two Sr OLCs.[35] $\mathrm{OFC_{chp}}$ works as an optical clockwork that transfers the frequency accuracy of the 698-nm Sr OLC to every comb modes covering wavelength range of 698 nm (OFSs' wavelength) and 1542 nm (transfer laser's wavelength). It needs to be mentioned that the 1542-nm comb mode is picked out from the leakage of the 698-nm output, thus resulting in a single-branch configura-

tion for the two beams. Multi-branch configuration would introduce excess differential noise, which could degrade the measurement stability to as high as $10^{-15}$ level in 1 s averaging time, owing to the independent uncompensated fiber systems.[36]

As shown in the upper panel of Fig. 2, the 698-nm laser beam from the clock laser of NIM-Sr2 goes through a noise-cancelled fiber link and combines with the output of $\mathrm{OFC_{chp}}$. The output of the 1542-nm transfer laser (CoSF-D-ER-M, Connet Laser Technology Co., Ltd.) passes through an AOM and is split into two parts by a fiber splitter. The two fiber pigtails of the splitter are centimeter-long and twisted together to reduce uncommon fiber noise. One part is combined with the 698-nm laser beam by a dichroic mirror (DM), and then combined with the 698-nm beam from $\mathrm{OFC_{chp}}$ at the beam splitter (BS). The combined beam is then split by the second DM. In this way, the 1542-nm transfer laser and the 698-nm clock laser beat with the adjacent comb modes (comb mode indexes are $n_{698,\mathrm{chp}}$ and $n_{1542,\mathrm{chp}}$) of $\mathrm{OFC_{chp}}$. The continuous wave (CW)-comb beat notes, $f_{\mathrm{b698,chp}}$ and $f_{\mathrm{b1542,chp}}$, are separately detected by two monochromatic detectors (DFC MD, TOPTICA). $f_{\mathrm{b698,chp}}$ is used to phase lock the corresponding comb modes of $\mathrm{OFC_{chp}}$ to the frequency of NIM-Sr, $\nu_{\mathrm{Sr2}}$, through pump current feedback (fast loop) and piezoelectric transducer (PZT) feedback (slow loop). $f_{\mathrm{b1542,chp}}$ is used to phase lock the 1542-nm transfer laser to the comb mode of 1542 nm in $\mathrm{OFC_{chp}}$. Here an external AOM (AOM1) is used as the fast actuator, and the PZT as the slow actuator.

The other part of the 1542-nm transfer laser is transferred to Hepingli campus through an urban telecommunication fiber link with active fiber noise cancellation, $\mathrm{FNC_{1542}}$. The fiber link that connects the two campuses is newly rented from a local telecommunications operator in 2023. Its length is measured to be 58 km by conventional optical time-domain reflectometer (OTDR) technique. A bidirectional Erbium-doped fiber amplifier is placed on Hepingli campus to counteract the $> 30$ dB power loss of the fiber link. A fiber AOM (AOM2) is installed after the amplifier to avoid unwanted reflection signals that are introduced by the nodes in the fiber link. A fiber Faraday rotator and a free space reference mirror (RM) act as a retro-reflector to reflect $< 10\%$ power of light back to Changping campus to beat with the local light (not transferred to Hepingli campus) for the fiber link noise cancellation. In order to evaluate the noise cancellation performance of $\mathrm{FNC_{1542}}$, an out-of-loop test is adopted by transferring the 1542-nm laser in a round trip between the two campuses utilizing two fiber cores in the same fiber link. Through the measurement of the instability of the beat between the local and the round-trip transferred light, the out-of-loop test characterizes the instability of $\sim 2\times10^{-16}$ at 1 s and better than $1\times10^{-18}$ at 10000 s for the 116 km fiber link.

$\mathrm{OFC_{hpl}}$ is a low noise commercial Er: fiber OFC (FC1500-250-WG, Menlo Systems). Its carrier-envelope offset, $f_{\mathrm{ceo,\,hpl}}$, is accessed by a conventional $f$-to-$2f$ interferometer. $f_{\mathrm{ceo,\,hpl}}$ is phase locked to a reference from a radio frequency synthesizer. Similar to the OFC on Changping campus, the comb mode (index $n_{698,\mathrm{hpl}}$) adjacent to the optical frequency of the NIM-Sr1, $\nu_{\mathrm{Sr1}}$, is phase locked to the 698-nm clock laser. This feedback utilizes the intracavity electro-optical modulator as the fast actuator while PZT as the slow actuator. After phase locking, the repetition frequency of $\mathrm{OFC_{hpl}}$, $f_{\mathrm{r,\,hpl}}$, is $\sim 250$ MHz. Similar to the comb on Changping campus, a single-branch 698/1542-nm output is built based on the 698 nm high-power measuring port (HMP698, Menlo Systems) to obtain the CW-comb beats, $f_{\mathrm{b698,hpl}}$ and $f_{\mathrm{b1542,hpl}}$, as shown in Fig. 2. A DM is placed at the free-space output to split the 698 nm and 1542 nm beams. The 698-nm beam from NIM-Sr1 clock laser is partly reflected by the RM for fiber noise cancellation ($\mathrm{FNC_{698,hpl}}$), combined with the comb beam by a BS and then directed to the free-space 698 nm beat detection unit (BDU) generating $f_{\mathrm{b698,hpl}}$. The 1542 nm laser transferred from Changping campus is combined with the 1542-nm comb by another BS, and then partly reflected by a RM for the 58-km fiber link noise cancellation enabled by $\mathrm{FNC_{1542}}$. The CW-comb beat, $f_{\mathrm{b1542,hpl}}$ is detected by a fiber-type 1542-nm BDU and counted by a dead-time-free frequency counter (FXE, K+K Messtechnik). Note that all the microwave frequency synthesizers and the frequency counters on the two campuses are referenced to the same radio reference generated from the same H-maser.

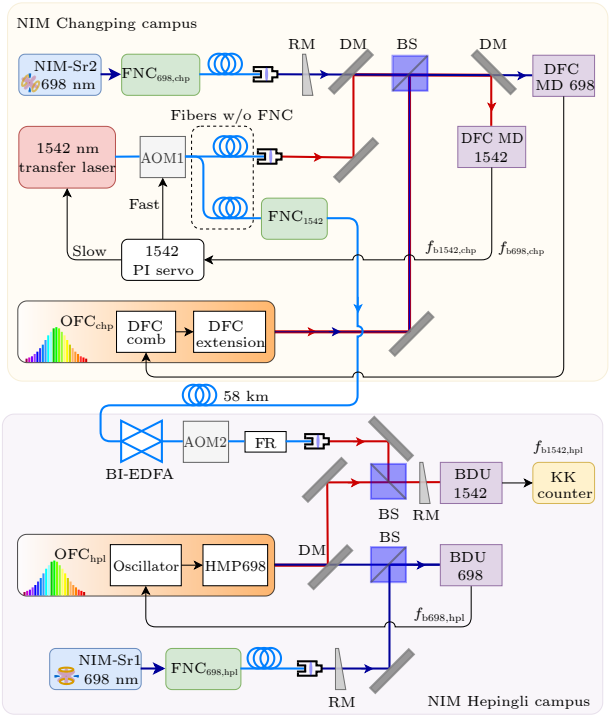


**Fig. 2.** The schematic of the frequency comparison chain. OFC: optical frequency comb; FNC: fiber noise cancellation; AOM: acousto-optic modulator; DFC: difference frequency generation; SHG: second harmonic generation; RM: reference mirror for fiber noise cancellation; DM: dichroic mirror; BS: beam splitter; MD: monochromatic detector; HMP: high power measuring port; BDU: beat detection unit; FR: fiber Faraday rotator; BI-EDFA: bidirectional erbium-doped fiber amplifer.

With the two Sr optical clocks, the OFCs and the

transfer links working, the equation for frequency difference between the two clocks can be derived. For $\mathrm{OFC_{chp}}$, because $f_{\mathrm{ceo,\,chp}}$ is zero, two comb equations are expressed as:

$$\begin{aligned}&\nu_{\mathrm{Sr2}} + f_{\mathrm{698AOM,chp}} + f_{\mathrm{FNC698,chp}}\\ &= n_{\mathrm{698,chp}}\cdot f_{\mathrm{r,chp}} + f_{\mathrm{b698,chp}},\end{aligned} \tag{1}$$

$$\begin{aligned}&\nu_{1542} + f_{\mathrm{phaselock}}\\ &= n_{\mathrm{1542,chp}}\cdot f_{\mathrm{r,chp}} + f_{\mathrm{b1542,chp}},\end{aligned} \tag{2}$$

where $\nu_{\mathrm{Sr2}}$ is the $^{87}$Sr clock transition frequency reproduced by NIM-Sr2, $f_{\mathrm{698AOM,\,chp}}$ is the frequency offset caused by the AOMs in NIM-Sr2, $f_{\mathrm{FNC698,chp}}$ is the frequency offset caused by $\mathrm{FNC_{698,chp}}$, $\nu_{1542}$ is the output frequency of 1542-nm transfer laser, and $f_{\mathrm{phaselock}}$ is the offset frequency in the phase lock of 1542 nm transfer laser.

For $\mathrm{OFC_{hpl}}$, the other two comb equations are expressed as:

$$\begin{aligned}&\nu_{\mathrm{Sr1}} + f_{\mathrm{698AOM,hpl}} + f_{\mathrm{FNC698,hpl}}\\ &= n_{\mathrm{698,hpl}}\cdot f_{\mathrm{r,hpl}} + 2f_{\mathrm{ceo,hpl}} + f_{\mathrm{b698,hpl}},\end{aligned} \tag{3}$$

$$\begin{aligned}&\nu_{1542} + f_{\mathrm{phaselock}} + f_{\mathrm{FNC1542}}\\ &= n_{\mathrm{1542,hpl}}\cdot f_{\mathrm{r,hpl}} + f_{\mathrm{ceo,hpl}} + f_{\mathrm{b1542,hpl}},\end{aligned} \tag{4}$$

where $\nu_{\mathrm{Sr1}}$ is the $^{87}$Sr clock transition frequency reproduced by NIM-Sr1, $f_{\mathrm{698AOM,\,hpl}}$ is the frequency offset caused by the AOMs in NIM-Sr1, and $f_{\mathrm{FNC698,hpl}}$ is the frequency offset caused by $\mathrm{FNC_{698,hpl}}$.

Substituting Eqs. (1)–(4) into $\Delta f_{\mathrm{Sr1-Sr2}} = \nu_{\mathrm{Sr1}} - \nu_{\mathrm{Sr2}}$, we arrive at

$$\begin{aligned}\Delta f_{\mathrm{Sr1-Sr2}} = {}& \frac{\left(n_{\mathrm{1542,chp}}n_{\mathrm{698,hpl}} - n_{\mathrm{1542,hpl}}n_{\mathrm{698,chp}}\right)\nu_{\mathrm{Sr2}} - n_{\mathrm{1542,chp}}n_{\mathrm{698,hpl}}f_{\mathrm{b698,chp}}}{n_{\mathrm{1542,hpl}}n_{\mathrm{698,chp}}}\\ &- \frac{n_{\mathrm{698,hpl}}\left(f_{\mathrm{ceo,hpl}} - f_{\mathrm{b1542,chp}} + f_{\mathrm{b1542,hpl}} + f_{\mathrm{AOMbias1}}\right)}{n_{\mathrm{1542,hpl}}} + 2f_{\mathrm{ceo,hpl}} + f_{\mathrm{b698,hpl}} - f_{\mathrm{AOMbias2}}.\end{aligned} \tag{5}$$

Some of the AOMs that are integrated in the OLCs and FNCs are not shown in Fig. 2. All the AOM setting frequencies cause the fixed bias frequency parts ($f_{\mathrm{AOMbias1}} = 12.5\,\mathrm{MHz}$ and $f_{\mathrm{AOMbias2}} = 103\,\mathrm{MHz}$) in Eq. (5). $f_{\mathrm{b698,chp}}$, $f_{\mathrm{b1542,chp}}$, $f_{\mathrm{b698,hpl}}$ and $f_{\mathrm{ceo,\,hpl}}$ are all phase locked to reference frequency synthesizers. All the AOM setting frequencies and phase lock reference frequencies are generated from frequency synthesizers. These synthesizers are referenced to 10-MHz $f_{\mathrm{ref,\,hpl}}$ or $f_{\mathrm{ref,\,chp}}$ that is delivered from the H-maser. With the type B frequency uncertainty of the H-maser better than $1\times10^{-14}$, these frequencies will not have an effect on the comparison uncertainties larger than $1\times10^{-19}$. The comb mode index $n_{\mathrm{698,chp}}$, $n_{\mathrm{1542,chp}}$, $n_{\mathrm{698,hpl}}$, $n_{\mathrm{1542,hpl}}$ can be calculated from the absolute frequencies of the 698-nm and 1542-nm lasers which are measured precisely with OFCs. We use the international recommendation value of the $^{87}$Sr clock transition as $\nu_{\mathrm{Sr2}}$,[37] which will not introduce an uncertainty larger than $1\times10^{-19}$ when the absolute frequency of NIM-Sr2 is better than $1\times10^{-13}$, because in Eq. (5), $\nu_{\mathrm{Sr2}}$ has a coefficient of $\sim 5\times10^{-7}$ when all comb mode indexes are substituted with their real values. The only unknown frequency is $f_{\mathrm{b1542,hpl}}$, which is measured by the frequency counter.

In 2021, after some major improvements, the systematic frequency shifts of NIM-Sr1 were re-evaluated.[31] Thereafter, NIM-Sr1 has been compared with UTC (NIM) intermittently, and the systematic frequency shifts have been updated with minor corrections according to the measured experimental parameters, as shown in Table 1.

**Table 1.** Frequency corrections and uncertainties of the two strontium optical lattice clocks.

| | NIM-Sr1 | | NIM-Sr2 | |
|---|---|---|---|---|
| Systematic effect | Correction ($10^{-17}$) | Uncertainty ($10^{-17}$) | Correction ($10^{-17}$) | Uncertainty ($10^{-17}$) |
| BBR MOT chamber | 491.9 | 1.6 | 506.28 | 0.37 |
| BBR oven and heated ZS window | 1.0 | 0.4 | 1.04 | 0.28 |
| Lattice scalar/tensor | 2.5 | 1.3 | 1.15 | 0.26 |
| Hyperpolarizability | −2.7 | 1.1 | −1.19 | 0.04 |
| Lattice M1/E2 | 0 | 0.6 | −2.01 | 0.08 |
| Collisions | 8.2 | 1.4 | 5.85 | 0.31 |
| 2nd Zeeman | 20.1 | 0.3 | 10.52 | 0.01 |
| Background gas collisions | 2.1 | 0.3 | 1.0 | 0.11 |
| DC Stark | 2.1 | 0.1 | 2.09 | 0.02 |
| Probe AC Stark | 0 | 0.1 | 0 | 0.1 |
| Servo error | 0 | 0.1 | 0 | 0.1 |
| Tunneling | 0 | 0.1 | 0 | 0.1 |
| Total | 525.2 | 2.9 | 524.73 | 0.65 |

NIM-Sr2 was evaluated in 2022.[27] After this evaluation, improvements have been made to reduce the BBR shift uncertainty. A passive thermal enclosure is installed around the MOT area. It mitigates the air flows passing the MOT chamber, and blocks direct thermal radiations from surrounding heat sources, which helps to improve the temperature uniformity of the thermal environment seen by the Sr atoms. The total systematic shift uncertainty is evaluated to be $6.5\times10^{-18}$,[38] as shown in Table 1.

In order to make frequency comparison of these two

Sr OLCs which are more than 40 km apart, relativistic redshift should be precisely evaluated. There is a leveling benchmark on Changping campus. Both the two labs' floor heights were measured relative to this leveling benchmark by the dimensional metrology laboratory of NIM.[31] The orthometric height difference of the MOT centers is evaluated to be 64.3(1) m, which will cause a fractional frequency shift of $-701.7(1.1)\times10^{-17}$ on $\Delta f_{\mathrm{Sr1-Sr2}}$.[31]

In March 2024, both Sr OLCs were regularly operated. Comparison data were taken from March 21. But on March 22, an unexpected but notified short term power outage occurred at Changping lab. Most devices of NIM-Sr2 were powered off during this power outage. Uninterruptible power supply kept critical parts of NIM-Sr2 operating, like vacuum pumps and temperature controllers for reference cavities, which helped NIM-Sr2 recover to normal operation within one week. About 43000 seconds of effective comparison data have been taken. The fractional instability of the comparison is shown in Fig. 3, analyzed using standard Allan deviation (ADev) with all the measurement data combined. The instability at 1 s is $5.7\times10^{-16}$, which is consistent with the combined instability of the two Sr OLCs and the transfer system. There is a bump in Fig. 3 at 2000 $\sim$ 3000 s, which coincides with the lab temperature regulation cycle time of Hepingli lab. The mechanism by which it is coupled to the comparison data needs further investigation. Weighted fit with a white frequency model, the instability follows $2.2\times10^{-15}/\sqrt{\tau}$. The ADev at 10000 s is $3.1\times10^{-17}$.

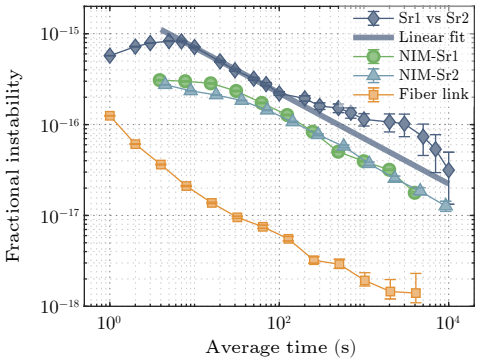


**Fig. 3.** The fractional instability of the comparison in terms of standard Allan deviation calculated based on all 4-day measurement data (dark blue curve, diamond). The dark-blue shaded line is the weighted fit using a white frequency noise model as $2.2\times10^{-15}/\sqrt{\tau}$. The remaining curves show the frequency instabilities of the fiber link and the time interleaved measurement of two Sr clocks.

$\Delta f_{\mathrm{Sr1-Sr2}}$ is calculated on a daily basis. The fractional frequency difference is shown in Fig. 4. The error bars in Fig. 4 are the 1 $\sigma$ combined measurement uncertainties, with type A measurement uncertainty, the Sr OLC systematic shift uncertainty, the relativistic redshift uncertainty and the frequency transfer uncertainty considered. The amber dashed line in Fig. 4 shows that the measurement result of the fractional frequency difference is $1.9\times10^{-17}$. The blue shaded region in Fig. 4 corresponds to the 1 $\sigma$ uncertainty, which is $3.2\times10^{-17}$.

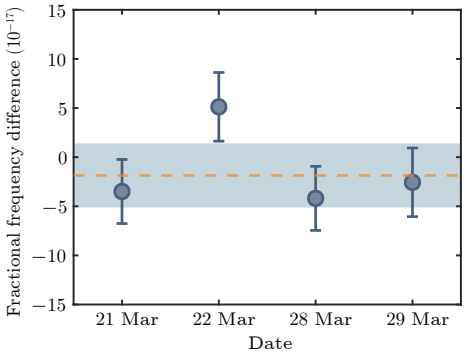


**Fig. 4.** The comparison result. The error bars indicate the 1 $\sigma$ combined measurement uncertainties on each day. The amber dashed line shows the fractional frequency difference between the two Sr OLCs. The blue shaded region corresponds to the 1 $\sigma$ uncertainty of the measured fractional frequency difference of all the data.

In summary, two Sr OLCs named NIM-Sr1 and NIM-Sr2 have been developed and operated at NIM. These OLCs are situated on separate NIM campuses with a distance of over 40 km. In order to realize frequency comparisons between these two Sr OLCs, a 58-km noise canceled fiber link transfers both a 1542-nm transfer laser and microwave reference from Changping campus to Hepingli campus. Two OFCs with single-branch type 698/1542 nm outputs coherently unite the clock lasers at 698 nm and the transfer laser at 1542 nm. The comparison result characterizes a fractional instability of $5.7\times10^{-16}$ and $3.1\times10^{-17}$, at 1 s and 10000 s average time, respectively. The measured fractional frequency difference between these two Sr OLCs is $1.9(3.2)\times10^{-17}$, which shows the consistency of the frequencies of these two Sr OLCs, and proves the validity of the clock systematic shift evaluations. Shortly after this measurement, NIM-Sr2 was moved to a new laboratory on Changping campus. We plan to make further frequency comparisons after the operation of NIM-Sr2 is recovered to help improve the systematic shift evaluations of both Sr OLCs. Replacing the fiber splitter in Fig. 2 with a spatial one would get rid of the non-common fiber in the setup. By reducing the uncertainty of the BBR shift, both NIM-Sr1 and NIM-Sr2 are expected to lower the uncertainty of systematic frequency shift. The plans for frequency comparisons with other types of OFSs would be proposed and further implemented in the future, to verify the frequency ratios to contribute to the redefinition of the SI second.

*Acknowledgements.* This work was supported by the National Key R&D Program of China (Grant No. 2021YFF0603802), the National Natural Science Foundation of China (Grant No. 61905231), the State Administration for Market Regulation (Grant No. CXTD202301), and the Innovation Program for Quantum Science and Technology (Grant No. 2021ZD0300902).

# References

[1] Chou C W, Hume D B, Koelemeij J C J, Wineland D J, and Rosenband T 2010 *Phys. Rev. Lett.* **104** 070802

[2] Hinkley N, Sherman J A, Phillips N B, Schioppo M, Lemke N D, Beloy K, Pizzocaro M, Oates C W, and Ludlow A D 2013 *Science* **341** 1215

[3] Bloom B J, Nicholson T L, Williams J R, Campbell S L, Bishof M, Zhang X, Zhang W, Bromley S L, and Ye J 2014 *Nature* **506** 71

[4] Nicholson T L, Campbell S L, Hutson R B, Marti G E, Bloom B J, McNally R L, Zhang W, Barrett M D, Safronova M S, Strouse G F, Tew W L, and Ye J 2015 *Nat. Commun.* **6** 6896

[5] Ushijima I, Takamoto M, Das M, Ohkubo T, and Katori H 2015 *Nat. Photon.* **9** 185

[6] Huntemann N, Sanner C, Lipphardt B, Tamm Chr, Peik E 2016 *Phys. Rev. Lett.* **116** 063001

[7] Brewer S M, Chen J S, Hankin A M, Clements E R, Chou C W, Wineland D J, Hume D B, and Leibrandt D R 2019 *Phys. Rev. Lett.* **123** 033201

[8] Zhang Z Q, Arnold K J, Kaewuam R, and Barrett M D 2023 *Sci. Adv.* **9** eadg1971

[9] Aeppli A, Kim K, Warfield W, Safronova M S, and Ye J 2024 *Phys. Rev. Lett.* **133** 023401

[10] Dimarcq N, Gertsvolf M, Mileti G, Bize S, Oates C W, Peik E, Calonico D, Ido T, Tavella P, Meynadier F, Petit G, Panfilo G, Bartholomew J, Defraigne P, Donley E A, Hedekvist P O, Sesia I, Wouters M, Dubé P, Fang F, Levi F, Lodewyck J, Margolis H S, Newell D, Slyusarev S, Weyers S, Uzan J P, Yasuda M, Yu D H, Rieck C, Schnatz H, Hanado Y, Fujieda M, Pottie P E, Hanssen J, Malimon A, and Ashby N 2024 *Metrologia* **61** 012001

[11] Rosenband T, Hume D B, Schmidt P O, Chou C W, Brusch A, Lorini L, Oskay W H, Drullinger R E, Fortier T M, Stalnaker J E, Diddams S A, Swann W C, Newbury N R, Itano W M, Wineland D J, and Bergquist J C 2008 *Science* **319** 1808

[12] Yamaguchi A, Fujieda M, Kumagai M, Hachisu H, Nagano S, Li Y, Ido T, Takano T, Takamoto M, and Katori H 2011 *Appl. Phys. Express* **4** 082203

[13] Takamoto M, Ushijima I, Das M, Nemitz N, Ohkubo T, Yamanaka K, Ohmae N, Takano T, Akatsuka T, Yamaguchi A, and Katori H 2015 *Comptes Rendus Physique* **16** 489

[14] Huang Y, Guan H, Liu P, Bian W, Ma L, Liang K, Li T, and Gao K 2016 *Phys. Rev. Lett.* **116** 013001

[15] Tyumenev R, Favier M, Bilicki S, Bookjans E, Targat R L, Lodewyck J, Nicolodi D, Coq Y L, Abgrall M, Guéna J, Sarlo L D, and Bize S 2016 *New J. Phys.* **18** 113002

[16] Lisdat C, Grosche G, Quintin N, Shi C, Raupach S M F, Grebing C, Nicolodi D, Stefani F, Al-Masoudi A, Dörscher S, Häfner S, Robyr J L, Chiodo N, Bilicki S, Bookjans E, Koczwara A, Koke S, Kuhl A, Wiotte F, Meynadier F, Camisard E, Abgrall M, Lours M, Legero T, Schnatz H, Sterr U, Denker H, Chardonnet C, Coq Y L, Santarelli G, Amy-Klein A, Targat R L, Lodewyck J, Lopez O, and Pottie P E 2016 *Nat. Commun.* **7** 12443

[17] Gao Q, Zhou M, Han C, Li S, Zhang S, Yao Y, Li B, Qiao H, Ai D, Lou G, Zhang M, Jiang Y, Bi Z, Ma L, and Xu X 2018 *Sci. Rep.* **8** 8022

[18] Dörscher S, Huntemann N, Schwarz R, Lange R, Benkler E, Lipphardt B, Sterr U, Peik E, and Lisdat C 2021 *Metrologia* **58** 015005

[19] Beloy K, Bodine M I, Bothwell T, Brewer S M, Bromley S L, Chen J S, Deschênes J D, Diddams S A, Fasano R J, Fortier T M, Hassan Y S, Hume D B, Kedar D, Kennedy C J, Khader I, Koepke A, Leibrandt D R, Leopardi H, Ludlow A D, McGrew W F, Milner W R, Newbury N R, Nicolodi D, Oelker E, Parker T E, Robinson J M, Romisch S, Schäffer S A, Sherman J A, Sinclair L C, Sonderhouse L, Swann W C, Yao J, Ye J, Zhang X, and Boulder (Atomic Clock Optical Network BACON Collaboration) 2021 *Nature* **591** 564

[20] Cao J, Yuan J, Wang S, Zhang P, Yuan Y, Liu D, Cui K, Chao S, Shu H, Lin Y, Cao S, Wang Y, Fang Z, Fang F, Li T, and Huang X 2022 *Appl. Phys. Lett.* **120** 054003

[21] Ma L S, Jungner P, Ye J, and Hall J L 1994 *Opt. Lett.* **19** 1777

[22] Lopez O, Haboucha A, Chanteau B, Chardonnet C, Amy-Klein A, and Santarelli G 2012 *Opt. Express* **20** 23518

[23] Chiodo N, Quintin N, Stefani F, Wiotte F, Camisard E, Chardonnet C, Santarelli G, Amy-Klein A, Pottie P E, and Lopez O 2015 *Opt. Express* **23** 33927

[24] Ohmae N, Sakama S, and Katori H 2019 *Electronics and Communications in Japan* **102** 43

[25] Schioppo M, Kronjäger J, Silva A, Ilieva R, Paterson J W, Baynham C F A, Bowden W, Hill I R, Hobson R, Vianello A, Dovale-Álvarez M, Williams R A, Marra G, Margolis H S, Amy-Klein A, Lopez O, Cantin E, Álvarez-Martínez H, Le Targat R, Pottie P E, Quintin N, Legero T, Häfner S, Sterr U, Schwarz R, Dörscher S, Lisdat C, Koke S, Kuhl A, Waterholter T, Benkler E, and Grosche G 2022 *Nat. Commun.* **13** 212

[26] Lin Y G, Wang Q, Li Y, Meng F, Lin B K, Zang E J, Sun Z, Fang F, Li T C, and Fang Z J 2015 *Chin. Phys. Lett.* **32** 090601

[27] Lu B K, Sun Z, Yang T, Lin Y G, Wang Q, Li Y, Meng F, Lin B K, Li T C, and Fang Z J 2022 *Chin. Phys. Lett.* **39** 080601

[28] Wang B, Gao C, Chen W L, Miao J, Zhu X, Bai Y, Zhang J W, Feng Y Y, Li T C, and Wang L J 2012 *Sci. Rep.* **2** 556

[29] Wang Q, Lin Y G, Li Y, Lin B K, Meng F, Zang E J, Li T C, and Fang Z J 2014 *Chin. Phys. Lett.* **31** 123201

[30] Li Y, Lin Y G, Wang Q, Yang T, Sun Z, Zang E J, and Fang Z J 2018 *Chin. Opt. Lett.* **16** 051402

[31] Lin Y G, Wang Q, Meng F, Cao S Y, Wang Y Z, Li Y, Sun Z, Lu B K, Yang T, Lin B K, Zhang A M, Fang F, and Fang Z J 2021 *Metrologia* **58** 035010

[32] Wang Q, Lin Y G, Gao F L, Li Y, Lin B K, Meng F, Zang E J, Li T C, and Fang Z J 2015 *Chin. Phys. Lett.* **32** 100701

[33] Shi H S, Lu B K, Zhang H Q, Hu R M, Qian Y, Huang Y, Yang T, Yao Y, Yu H F, Fang Z J, Gao K L, Guan H, Lin Y G, Jiang Y Y, and Ma L S 2024 *Photonics Res.* **12** 2741

[34] Zhang H Q, Huang Y, Zhang B L, Hao Y M, Zeng M Y, Chen Q F, Wang Y Z, Cao S Y, Lin Y G, Fang Z J, Guan H, and Gao K L 2023 *Metrologia* **60** 035004

[35] Tian H C, Cai Y, Yang T, Wang Q, Wang X Q, Lin B K, Meng F, Li Y, Fang Z J, Steinmeyer G, and Lin Y G 2024 *Appl. Phys. Lett.* **125** 241107

[36] Nakajima Y, Inaba H, Hosaka K, Minoshima K, Onae A, Yasuda M, Kohno T, Kawato S, Kobayashi T, Katsuyama T, and Hong F L 2010 *Opt. Express* **18** 1667

[37] Nemitz N, Ohkubo T, Takamoto M, Ushijima I, Das M, Ohmae N, and Katori H 2016 *Nat. Photon.* **10** 258

[38] Yang T, Lu B, Zhu L, Liao T, Wang Q, Li Y, Meng F, Lin B, Wang Y, Fang F, Lin Y, and Fang Z 2024 *J. Phys.: Conf. Ser.* **2889** 012047